Impact of Self-Phase Modulation on Instabilities in Fiber Lasers

Hojoon Lee, *Senior Member, IEEE* and Govind P. Agrawal, *Fellow, IEEE*

***Abstract*— Continuously pumped Yb-doped double-clad fiber lasers exhibit two kinds of instabilities, known as self-sustained pulsing and self-mode locking (SML). We study numerically the role of self-phase modulation (SPM) on the onset of these stabilities by using a spatiotemporal model that takes into account fully the length dependence of both the optical gain and spontaneous emission, while also including the nonlinear effects within the fiber. Self-sustained pulsations originate from relaxation oscillations. Although they die out quickly in the absence of SPM, our results show that SPM restores these oscillations when the laser power exceeds a certain value. SML has its origin in the spontaneous-emission noise acting as a seed. The laser cavity amplifies this noise the most at frequencies associated with its longitudinal modes, resulting in periodic power variations with an amplitude <1% (without SPM). We find that SPM plays again a critical role and increases their amplitude to above the 10% level. We also show that the SPM-induced instabilities can be suppressed by inserting a passive fiber of suitable length inside the laser cavity, which is in agreement with recent experimental work.**

***Index Terms*— Laser stability, nonlinear wave propagation, optical fiber lasers, ytterbium lasers.**

I. Introduction

FIBER lasers are used for many applications such as free-space communications, spectroscopy, medical optics, and fiber sensors [1]. In the case of high-power applications, a double-clad fiber with a single-mode core is used, rather than a standard single-clad fiber, because considerable pump power can be coupled into its outer cladding using broad-stripe laser diodes. Optical gain is provided by a rare-earth material doped into the fiber core. In particular, ytterbium ions (Yb^{3+}) have a broad absorption peak in the wavelength region near 920 nm, which can be used for pumping such lasers with commercially available low-cost laser diodes. Moreover, Yb^{3+} ions form effectively a simple two-level system that helps in avoiding excited-state absorption for both the pump and laser light. These characteristics result in relatively high slope efficiencies for Yb-doped fiber lasers (YDFL) [2]. A large spectral bandwidth of fluorescence in such lasers is useful for tunable applications.

Several instabilities have been reported when a YDFL is pumped continuously and designed to emit continuous wave (CW) radiation near 1060 nm. Two instabilities are known as sustained self-pulsing (SSP) and self-mode locking (SML) [3]. SSP results in emission of pulses at a repetition rate that is associated with relaxation oscillations and is typically much smaller ($\sim$0.1 MHz) than the spacing of longitudinal modes related inversely to the cavity round-trip time (typically $>$1 MHz). SSP can be observed in a specific pumping range under typical cavity-design conditions. SML is related to the onset of multiple longitudinal modes and results in output pulses with a period exactly equal to the cavity round-trip time.

In earlier work, such instabilities were identified as resulting from saturable absorption from ion pairing in heavily Er-doped or Tm-doped fibers [4], [5]. It was pointed out later that instabilities can also result from nonlinear dynamics of the laser signal and atomic populations in various energy states [6]–[8]. A simple model describing SML and SSP instabilities in a unidirectional ring-fiber laser was proposed in 2005 using only the interaction between the saturated population inversion and optical signal circulating inside the laser cavity [9]. It is based on the repetitive amplification of an optical pulse circulating in the cavity with homogeneous gain saturation. This model explains the SML behavior close to laser threshold followed with a sharp transition to the SSP regime. It agrees qualitatively with experiments, although the predicted pumping level at which transition occurs is much higher than that observed experimentally.

A qualitative analysis of SML in Er-doped fiber lasers was carried out in 1995 using Maxwell–Bloch equations [3]. This approach has also been used for YDFLs [10]. It shows that SML starts as low-amplitude sinusoidal modulations that take the form of intense short pulses because of the onset of multiple nonlinear effects such as stimulated Brillouin scattering, stimulated Raman scattering and self-phase modulation.

Two different techniques have been used to reduce self-pulsing instabilities in YDFLs. The end-pumped geometry, in which pump light is coupled into the fiber core at one end, leads to the existence of a high-absorption region near the far end at low pump levels. It is reported that a YDFL with a short fiber length, or with double-end pumping, becomes more stable because of a reduced unpumped fiber length and the resulting reduced saturated absorption [11]. Recently, a new method for suppressing self-pulsing in a double-clad YDFL was reported [12]. In this approach, the addition of a long

Manuscript received November 9, 2009; revised May 13, 2010 and June 11, 2010; accepted July 7, 2010. Date of current version October 6, 2010.

H. Lee was with the Institute of Optics, University of Rochester, Rochester, NY 14627 USA. He is now with the Department of Information Communication, Hoseo University, Asan 336-795, South Korea (e-mail: hojoon @hoseo.edu).

G. P. Agrawal is with the Institute of Optics and Department of Physics and Astronomy, University of Rochester, Rochester, NY 14627 USA (e-mail: gpa@optics.rochester.edu).

Color versions of one or more of the figures in this paper are available online at http://ieeexplore.ieee.org.

Digital Object Identifier 10.1109/JQE.2010.2063416

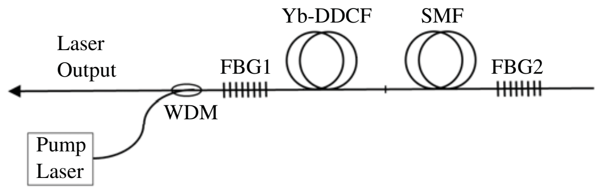

Fig. 1. Schematic of a CW double-clad YDFL. (FBG: fiber Bragg gratings, SMF: single-mode fiber, WDM: wavelength division multiplexing, and DDCF: doped double-clad fiber.)

section of passive fiber within the laser cavity makes the gain recovery faster than the self-pulsation dynamics, allowing only stable CW lasing.

In this paper, we study numerically the role of SPM on the onset of laser stabilities by using a spatiotemporal model that takes into account fully the length dependence of both the optical gain and spontaneous emission, while also including the nonlinear effects within the fiber. Both the SML and SSP instabilities are investigated using this model through numerical simulations. This paper is organized as follows. In Section II, we introduce the theoretical model and describe the coupled mode equations, atomic rate equations, and the boundary conditions that govern a YDFL system. Solving these equations numerically, we discuss in Section III, the SSP and SML instabilities and show that SPM affects both of them considerably. In Section IV, we show that the instabilities can be suppressed by inserting a passive fiber of suitable length inside the laser cavity. We summarize our results and conclusions in Section V.

II. Theoretical Model and Laser Parameters

We focus on a Fabry–Perot cavity consisting of a doped fiber of length L that is surrounded by two FBG acting as mirrors. Such a laser is sometimes called a distributed Bragg reflector fiber laser. Fig. 1 shows the schematic of the laser cavity considered in this paper. A pump laser launches 920 nm radiation into the core of the double-clad fiber doped uniformly with Yb to provide gain [13]. Two FBG have reflectivities of $R_1 = 4\%$ and $R_2 = 99\%$ over a 0.5 nm bandwidth centered at 1090 nm. The nonlinear effects inside fibers are included by assuming that the effective refractive index of the fundamental mode of the fiber varies with intensity as

$$n(z) = \overline{n} + n_2 \left|E(z)\right|^2 \tag{1}$$

where $\overline{n}$ is the linear part of the effective mode index and n_2 is the nonlinear-index coefficient with a value of 2.6×10^{-20} m^2/W [17]. The frequency dependence or dispersion of $n(z)$ is ignored in this paper since it becomes important only for very short pulses (width 1 ps or less) for typical fiber lengths used for YDFLs.

To analyze the performance of a fiber laser, two approaches have been employed. In a simple approach [14], [15], all variables depend on time but not on the distance z within the fiber. This method obtains the temporal shape of the emitted pulse by solving two coupled rate equations governing density of photons in the cavity and the density of excited ions. Although such a method is quite successful, it fails to provide quantitative agreement with the experiments because of its neglect of longitudinal variations of all quantities along the fiber length. For this reason, we employ the traveling-wave method that takes into account longitudinal variations fully [16].

To describe the laser dynamics, we employ the notation of [17] and write the optical field appearing in (1) as

$$\begin{aligned} E(z,t) = \mathrm{Re}\Big\{ &\sqrt{P_p(z,t)/A_e}\cdot \exp[i(k_p z - \omega_p t)] \\ &+ E_s^+(z,t)\exp[i(k_s z - \omega_0 t)] \\ &+ E_s^-(z,t)\exp[-i(k_s z + \omega_0 t)]\Big\} \end{aligned} \tag{2}$$

where $A_e = n_g A_{eff}/(2Z_0)$, n_g is the group index, A_{eff} is effective mode area of the optical fiber, Z_0 is characteristic impedance of vacuum, $P_p(z,t)$ is the pump power, and ω_p and ω_0 are the angular frequencies of the pump and laser signal, respectively. The laser (or signal) fields $E_s^{\pm}(z,t)$ propagating in both the forward and backward directions are included because of reflections provided by the two gratings.

Our numerical analysis is based on a rate-equation model. It includes transitions such as stimulated emission, absorption, and spontaneous emission at the laser wavelength and stimulated emission and absorption at the pump wavelength [13]. In the slowly varying envelope approximation, we solve the following set of coupled nonlinear partial differential equations [18]–[20]:

$$\begin{aligned} \pm\frac{\partial E_s^{\pm}}{\partial z} + \frac{1}{v_g}\frac{\partial E_s^{\pm}}{\partial t} &= i\gamma\left(\left|E_s^{\pm}\right|^2 + 2\left|E_s^{\mp}\right|^2\right)E_s^{\pm} \\ &\quad + \Gamma_s/2\cdot(\sigma_{es}N_2 - \sigma_{as}N_1)E_s^{\pm} + f_{sp}^{\pm} - \alpha_s/2\cdot E_s^{\pm} \end{aligned} \tag{3}$$

$$\pm\frac{\partial P_p}{\partial z} + \frac{1}{v_g}\frac{\partial P_p}{\partial t} = \Gamma_p[\sigma_{ep}N_2 - \sigma_{ap}N_1]P_p - \alpha_d P_p \tag{4}$$

$$\begin{aligned} \frac{\partial N_2}{\partial t} = &-\frac{N_2}{\tau_{21}} - \frac{\lambda_p\Gamma_p}{hcA_{eff}}\left(\sigma_{ep}N_2 - \sigma_{ap}N_1\right)P_p \\ &- \frac{n_g\lambda_s\Gamma_s}{2hcZ_0}\left(\sigma_{es}N_2 - \sigma_{as}N_1\right)\left(E_s^{+^*}E_s^{+} + E_s^{-^*}E_s^{-}\right) \end{aligned} \tag{5}$$

$$N_1 = N_0 - N_2 \tag{6}$$

where $v_g = c/n_g$ is the group velocity, c is the velocity of the light in vacuum, $\gamma = n_2\omega_0/(cA_{eff})$ is nonlinear parameter, and α_s and α_p are the fiber loss coefficients at the signal and pump wavelengths, respectively. The interaction of light with Yb ions is described by (5) and (6), where N_1 and N_2 are the ion densities in the ground and excited states, respectively, and N_0 is the dopant density in the fiber core. Further, τ_{21} is the upper-state lifetime, σ_{as}, σ_{es}, σ_{ap} and σ_{ep} denote the absorption and emission cross sections at the signal and pump wavelengths, and Γ_s and Γ_p provide a measure of the overlap of the optical modes with the dopants.

Since any laser starts from spontaneous emission, it must be included in any realistic laser model. We include it in (1) through the $f_{sp}(z,t)$ term which acts as a Langevin noise source. Amplified spontaneous emission (ASE) builds from

TABLE I
YDFL PARAMETERS USED IN NUMERICAL SIMULATIONS

$n_g = 1.46$	
$\gamma_p = 0.92\ \mu$m	$A_{eff} = 5 \times 10^{-11}$ m^2
$\gamma_s = 1.09\ \mu$m	$\alpha_{s(SMF)} = 4.6 \times 10^{-4}$ m^{-1}
$\tau_{21} = 0.84 \times 10^{-3}$ s	$\alpha_p = 5 \times 10^{-3}$ m^{-1}
$N_0 = 1.9 \times 10^{25}$ m^{-3}	$\alpha_s = 2.3 \times 10^{-3}$ m^{-1}
$\sigma_{ap} = 7.8 \times 10^{-25}$ m^2	$\Gamma_s = 0.82$
$\sigma_{ep} = 3 \times 10^{-26}$ m^2	$\Gamma_p = 0.0012$
$\sigma_{as} = 1.2 \times 10^{-27}$ m	$\Delta\gamma_s = 0.5$ nm
$\sigma_{es} = 1.8 \times 10^{-25}$ m^2	$L = 20$ m

this noise seed taken to be a Markovian–Gaussian random process with the moments

$$\langle f_{sp}(z,t)\rangle = 0, \quad \langle f_{sp}(z,t) f_{sp}(z',t')\rangle = F\delta(z-z')\delta(t-t') \tag{7}$$

where $F = 2h\upsilon\Gamma_s\sigma_{es}N_2/A_e$ governs the magnitude of the spontaneous emission into the laser mode (the factor of two results from the two polarization components of ASE). This quantity is time and space dependent because of its dependence on $N_2(z,t)$. We include ASE by taking f_{sp} in the form of a random complex number whose magnitude depends on F.

An iterative solution of (3)–(6) is obtained numerically using the fourth-order Runge–Kutta method with the initial conditions $P_p(z=0,t) = P_{p0}(t)$, $E_s^+(z,t=0) = 0$, $E_s^-(z,t=0) = 0$ and the following boundary conditions at the left and right ends ($z = 0$ and L) of the laser cavity:

$$E_s^+(0,t+\Delta t) = r_1\sqrt{\alpha_c}E_s^-(0,t) \tag{8}$$

$$E_s^-(L,t+\Delta t) = r_2\sqrt{\alpha_c}E_s^+(L,t) \tag{9}$$

$$P_p^+(0,t+\Delta t) = P_{p0}(t) \tag{10}$$

$$P_p^-(L,t+\Delta t) = 0 \tag{11}$$

where $R_1 = r_1^2$ and $R_2 = r_2^2$ are the grating reflectivities and α_c is related to losses resulting from the splicing of FBG to the Yb-doped fiber. The round-trip cavity loss, in addition to fiber losses, is taken to be 3 dB ($\alpha_c = 0.5$). Values of physical parameters used in our simulations are shown in Table I. The absorption and emission cross sections of the Yb-doped fiber are from [21]. In all simulations, the pump power $P_{p0}(t)$ builds up from 0 to its maximum value with a rise time (10 to 90% of the peak) of 100 ns.

III. SSP AND SML INSTABILITIES

For the parameter values listed in Table I, the YDFL reaches threshold at a pump power of about 0.33 W. Below this threshold level, the output power, $P_0(t) = A_e|E_s^-(0,t)|^2\alpha_c(1-R_1)$, is relatively weak and consists of ASE only. When pump power exceeds the threshold level, the laser power begins to build up rapidly with an initial time delay that depends on how far above threshold the laser is pumped. We define the pumping level as a ratio of the pump power to its threshold value ($r = P_p/P_{th}$).

Fig. 2 shows how output power builds up when the laser is pumped close to its threshold ($r = 1.2$). It shows an initial

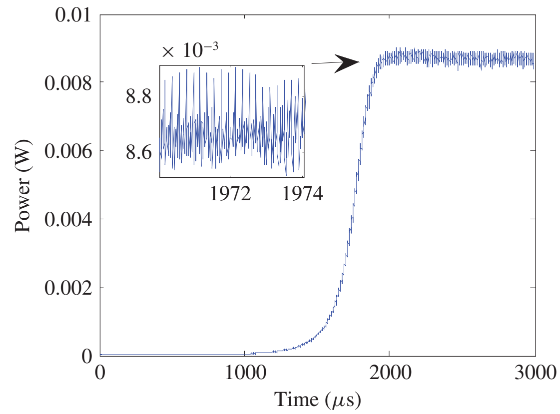

Fig. 2. Output characteristics at a pump power of 0.4 W ($r = 1.2$).

delay of about 1500 μs before the laser power reaches its steady-state value of about 8.7 mW. However, the laser output exhibits considerable power variations at a frequency that is related to the SML instability, as shown in the inset of Fig. 2. This behavior has been seen in previous work [3], [9]. For example, in the experiment reported in [9], such low-power SML was observed in the range $1 < r < 3.3$. It should be stressed that SPM plays virtually no role in Fig. 2 because intracavity power is too small to cause significant nonlinear phase shifts. We find that SPM becomes significant for $r > 2$, and its effects should be included.

When r exceeds 2.3, we enter the SSP regime in which the laser exhibits self-pulsing at the frequency of relaxation oscillations. Fig. 3 shows the impact of SPM on output power evolution for $r = 3$ ($P_p = 1$ W). The upper row in this figure shows the output characteristics when we intentionally turn off the nonlinear effects (mainly SPM) by setting $\gamma = 0$. The bottom row shows how the output changes when the nonlinear effects are included. In both cases, there is an initial delay of about 350 μs before the laser turns on, and after that the laser exhibits self-pulsing with a period of about 28 μs [see Fig. 3(a) and (d)]. The main difference is that relaxation oscillations quickly die out and laser power becomes constant when $\gamma = 0$. In contrast, temporal pulsations continue indefinitely when γ is finite and they appear to contain several frequencies.

To understand the laser behavior in more detail, we show in Fig. 3(b) the spectrum of power variations by taking the Fourier transform of $P_0(t)$ in the entire 1-ms-wide time window. The spectral peaks at multiples of 1 kHz results from this finite 1-ms window and should be ignored. The broad peak around 35 kHz in the power spectrum is due to relaxation oscillations. The phasor plot of the output field is shown in (c) by plotting the real and imaginary parts of the electric fields along the x- and y-axes, respectively, at times >0.9 ms. It shows clearly that nearly coherent light is generated by the laser with some amplitude and phase fluctuations.

We now consider the impact of SPM on laser power in more detail. Temporal pulsations in Fig. 3(d) contain more than one frequency. The power spectrum in (e) shows that, in addition to the relaxation-oscillation peak at 35 kHz, several peaks occur at multiples of a frequency close to 5 MHz. This frequency

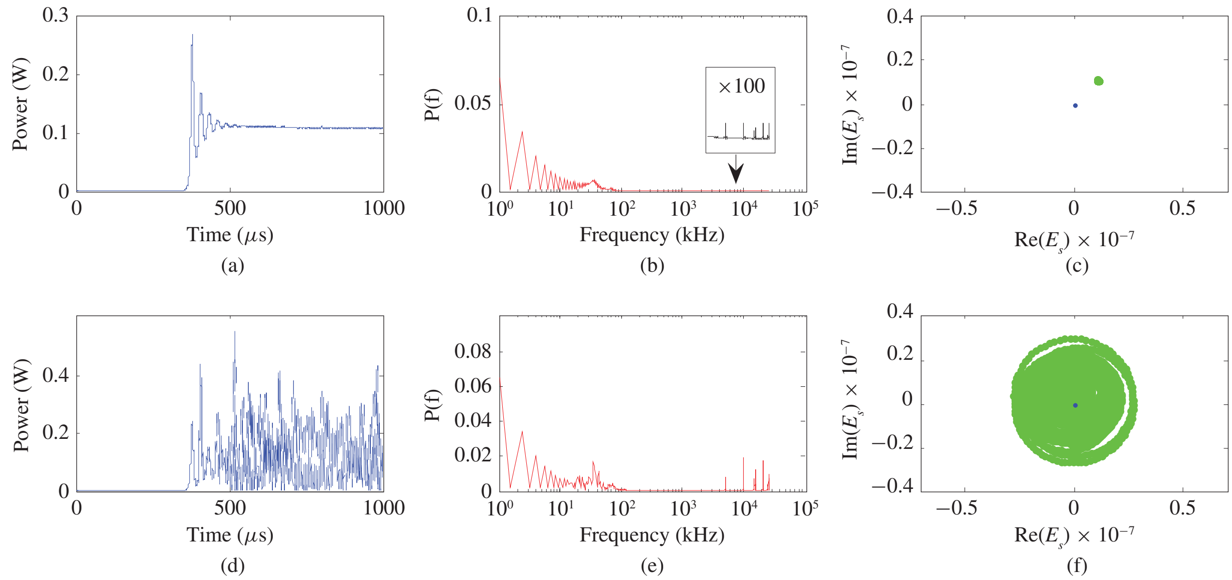

Fig. 3. Output characteristics of a YDFL at a pump power of 1 W ($r = 3$) without SPM (upper row) and with SPM (lower row). Power variations with time (left column), the resulting power spectrum (middle column), and phasor diagram of the laser field for the final 20% of time window (right column).

matches the round-trip frequency $\Delta\nu = v_g/2L$, where $v_g = c/n_g$ is the group velocity. It thus appears that SPM leads to SML of our YDFL. However, before reaching this conclusion, we should ask whether these frequencies are present in (b) where SPM is ignored by setting $\gamma = 0$. Indeed, we find that SML occurs even in this situation but the amplitude of SML peaks is so small that output power varies by less than 0.1% during each round-trip time. This is the reason why laser power appears virtually constant after 0.5 ms in (a). We thus conclude that ASE is the true origin of SML but SPM plays an important role by enhancing the amplitude of SML spectral peaks so that the output takes the form of pulsations at the round-trip frequency. Indeed, if we use a constant field with no fluctuations to seed the growth of laser output, SML disappears. Because of the important role played by ASE, the exact temporal form of SML pulses is not predictable. The phase diagram in (f) confirms that the laser emits light with severe amplitude and phase variations induced by ASE and enhanced by SPM.

Fig. 4 shows the temporal evolution of laser output at a pump power of 2.5 W ($r = 7.6$). The behavior is similar to that seen in Fig. 3(d) for $r = 3$ except that a few giant pulses are emitted before the SML region is stabilized. An important question is how much the behavior changes when laser is pumped much above threshold to obtain high powers. We have changed the pumping level r over a wide range extending from $r = 0.5$ to 50. The SML instability occurred for our YDFL in the pump power range from 0.5 to 14 W (or $r = 1.5$ to 42). Beyond $r = 42$, the self-pulsing disappears, and the laser output becomes relatively constant except for low-amplitude power fluctuations. Fig. 5 shows this behavior under conditions identical to those of Fig. 2 except that r is close to 45 at a pump power of 15 W. As before, SPM is ignored for results shown in the upper row but is included in the bottom row. As expected on physical grounds, the relaxation-oscillation frequency is higher in this high-power case compared with the case of 1 W pump power. The power spectrum in Fig. 5(b)

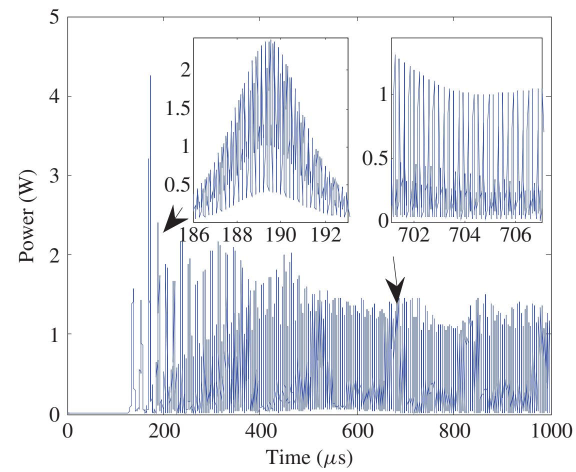

Fig. 4. Output characteristics at a pump power of 2.5 W ($r = 7.6$).

reveals this frequency to be around 145 kHz. SML peaks are also very weak as seen from the inset, where they have been magnified by a factor of 50. In the absence of SPM, the phasor diagram in Fig. 5(c) shows a relatively small circle, indicating that the laser emits well-stabilized coherent light with relatively small power and phase fluctuations.

The bottom part of Fig. 5 shows how this behavior is affected by SPM. Temporal power variations in Fig. 5(d) shows that, in contrast to the low-power case depicted in Fig. 3, the laser is not destabilized by SPM because the laser power becomes nearly constant after 0.2 ms, without exhibiting large-amplitude self-pulsing. However, this does not mean that SML does not occur. The power spectrum in Fig. 5(e) exhibits several peaks at multiples of $\Delta\nu$ whose amplitude has been enhanced by SPM, but the enhancement is reduced considerably compared with the low-power case. The phase diagram in Fig. 5(f) shows a donut-shape pattern and indicates that the extent of power and phase fluctuations. The reason that

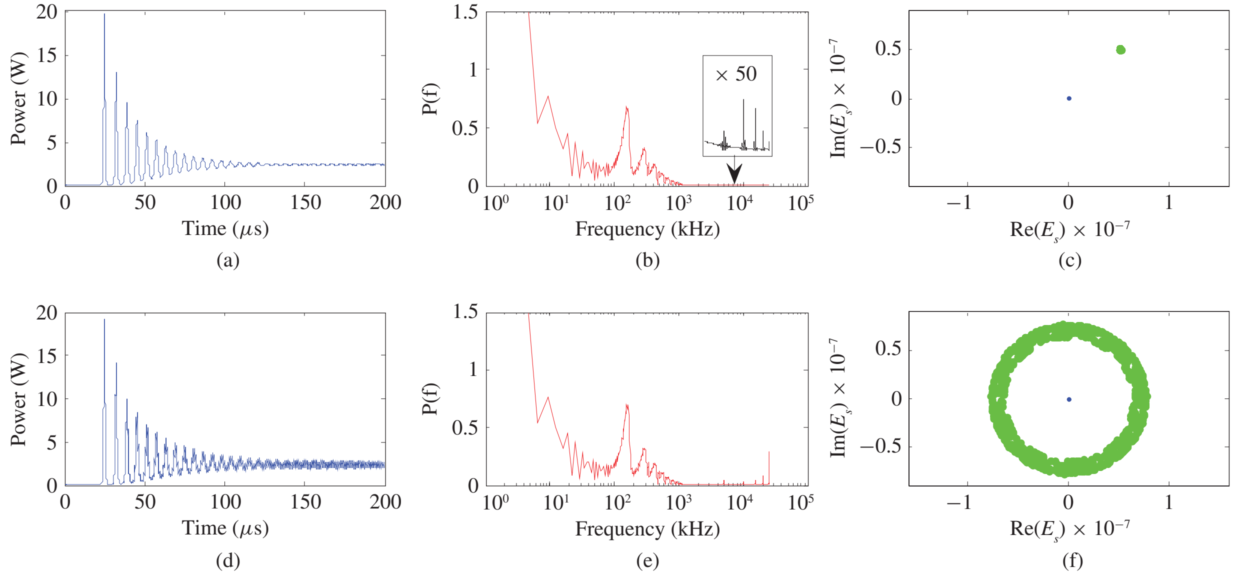

Fig. 5. Same as Fig. 3 except that the pump power has been increased to 15 W ($r = 45$).

TABLE II
MEASURED AND CALCULATED PUMPING RATIOS FOR THE FOUR DYNAMIC REGIMES

	Measured pumping ratio [9]	Calculated pumping ratio [9]	Calculated pumping ratio in this paper
Low-power SML	$1 < r < 3.3$	$1 < r < 23$	$1 < r < 2.3$
SSP	$3.9 < r < 4.6$	$25 < r < 70$	$2.4 < r < 7.0$
High-power SML	$r > 6.4$	$r > 80$	$7.6 < r < 42$
Stable			$r > 43$

a circle in Fig. 3(f) has been transformed into a donut is related to a shift in the laser frequency induced by SPM. Because of phase shift induced by SPM over each round trip, the laser can attain a steady state only if it shifts its frequency by a certain amount. The main conclusion that can be drawn from Fig. 5 is that a YDFL is stabilized at high pumping levels to the extent that even SPM is unable to destabilize it.

Table II compares the range of r for the three instability regimes predicted by our model with that predicted by the simple model of [9]. Also shown are the experimental values from [9]. It is evident that our model provides a much better agreement even though we did not attempt to match the laser design or its cavity parameters. In fact, a ring cavity was used in [9], whereas our simulations are done for a Fabry–Pertot cavity.

IV. Control of Laser Instabilities

From a practical perspective, instabilities are not desirable for CW lasers intended to provide a constant output power after transients have died out. As mentioned earlier, it was found in a recent experiment [12] that the addition of a long section of passive fiber within the laser cavity suppresses SSP and SML instabilities in a double-clad YDFL. We have followed this approach and have studied numerically how the instability range of pump power depends on the length of passive SMF section by changing this length in the range of 0 to 1000 m. As an example, the output characteristics of our YDFL with a 1000-m section of passive fiber in the cavity is shown in Fig. 6. As in Figs. 3 and 5, we show the output power as a function of time in the left column, the power spectrum in the middle column, and the phasor diagram in the right column at pump powers of 1 W (upper row) and 15 W (lower row). The nonlinear effects are fully included in all cases.

Several features are noteworthy in Fig. 6. First, the laser exhibits damped relaxation oscillations and its output power becomes nearly constant (with considerable noise) after a few milliseconds at both 1 W and 15 W pumping levels. The power spectrum shows that the relaxation oscillation frequencies are 5 and 21 kHz at pump powers of 1 and 15 W, respectively. The SML signature frequencies corresponding to the cavity round-trip time are still present, but the round-trip time of 10 μs results in a longitudinal mode spacing of only 100 kHz because of the 1-km-long passive fiber section inside the cavity. The extent of power and phase fluctuations is evident in the phasor diagrams in Fig. 6, which shows a donut shape that is a characteristic of stable operation with a shaded region whose width indicates the noise level. The main point to emphasize is that the laser operates in a stable manner over the entire range of pump powers.

An important practical question is how long the passive section should be because one should use the shortest possible length to avoid additional cavity losses. We use the level of relative noise variance as a measure of the laser stability, it is defined as the ratio σ^2/P_{av}^2 where σ^2 is the power variance and P_{av} is the average power. Fig. 7 shows the color-coded relative noise variance as contours in a 2-D plane showing the length of intracavity passive fiber along the x-axis and the pump power along the y-axis. When no SMF is used inside the cavity, the instability regime is quite wide extending from 0.8 to 9.5 W of pump power. For a 100-m-long fiber

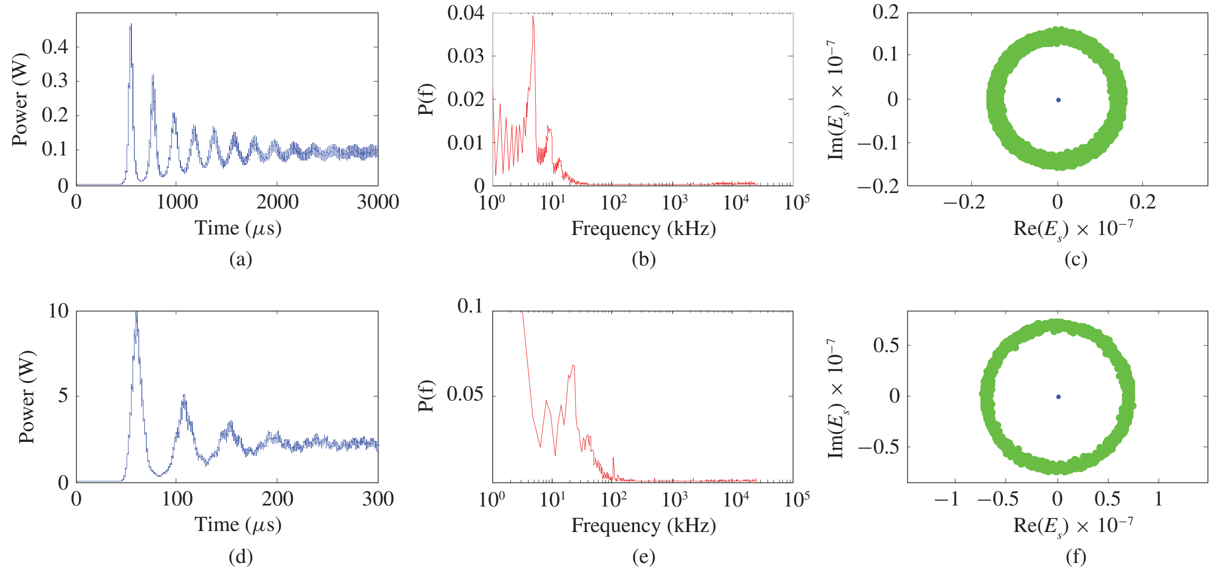

Fig. 6. Output characteristics of a YDFL with 1-km-long passive fiber section used to control instabilities. Different parts show output power as a function of time (left column), power spectrum (middle column), and the phasor diagram (right column) at pump powers of 1 W (upper row) and 15 W (lower row).

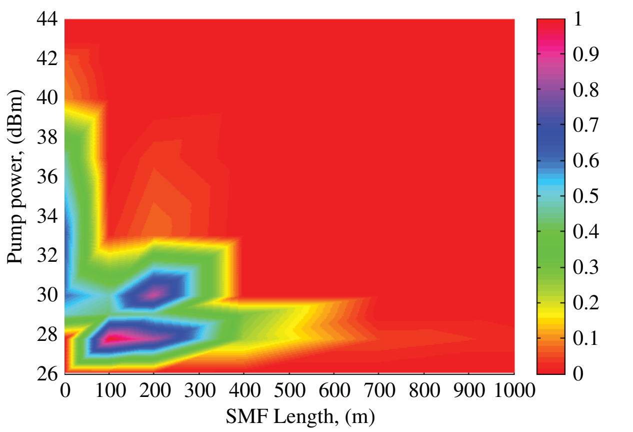

Fig. 7. Color-coded relative noise variance as contours in a 2-D plane showing length of intracavity passive fiber along the x-axis and applied pump power along the y-axis. Splicing loss between the FBG and Yb-doped fiber is 30% ($\alpha_c = 0.7$).

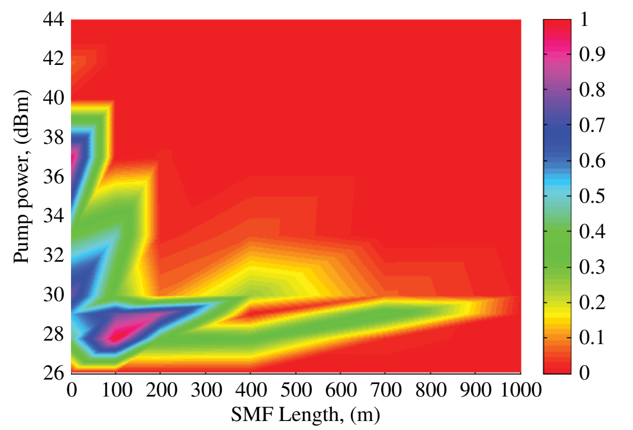

Fig. 8. Same as Fig. 5 except the splicing loss between the FBG and Yb-doped fiber is 10% ($\alpha_c = 0.9$).

section, the instability regime is changed to 0.4–1.7 W (26–32.3 dBm), resulting in a stable operation of the laser at pump powers exceeding 1.8 W. Further reduction in the instability range occurs for fiber lengths of 400 m or more, and the laser becomes nearly stable at all pumping levels when the fiber length exceeds 700 m. The required length of passive fibers depends on several other laser parameters. As an example, Fig. 8 shows the instability range under conditions identical to those of Fig. 5, except that the cavity loss per pass is reduced to 10%. As seen there, in this case instability can be suppressed only when the length of passive fiber exceeds 1000 m.

The important question is what physical mechanism is responsible for suppression of instabilities. It has been argued [12] that the addition of a long section of passive fiber makes the gain recovery faster than the self-pulsation dynamics, allowing for stable CW lasing. This argument makes sense. Indeed, the damping time of relaxation oscillations is given by $T_{RO} = \tau_{21}/r$, where r is the pumping level. The cavity lifetime, $\tau_c = T_{RT}/l_T$, is related to both the round-trip time T_{RT} and total round-trip losses inside the cavity. At a pumping level of 1 W ($r = 3$), T_{RO} of 270 μs is much longer than τ_c but at a pumping level of 15 W ($r = 45$), it is reduced to below 20 μs. When a 1-km-long passive fiber is employed, T_{RL} increases to 10 μs, and τ_c becomes 0.1 ms for 10% round-trip losses. Now, the laser becomes stable at all pumping levels because the gain-recovery time becomes a fraction the cavity lifetime.

V. Conclusion

Continuously pumped Yb-doped double-clad fiber lasers exhibit two kinds of instabilities, known as self-sustained pulsing and SML. We studied numerically the role of SPM on the onset of these instabilities by using a spatiotemporal model that takes into account fully the length dependence of both the optical gain and spontaneous emission, while also including the nonlinear effects within the fiber. Relaxation oscillations, which are intrinsic to any oscillator, normally die out quickly. This is also the case for a fiber laser in the absence of SPM because both the dopant density and the laser power reach a steady state in that situation. However, our results showed that SPM makes relaxation oscillations self-sustaining (resulting in SSP) when the laser power exceeds a certain value because of a relatively large phase shift induced by the SPM.

SML has its origin in the spontaneous-emission noise that seeds the buildup of the laser power. The laser cavity amplifies this noise the most at frequencies associated with its longitudinal modes, resulting in periodic power variations with an amplitude <1% (without SPM). We found that SPM plays again a critical role and increases their amplitude to above 10%. We also showed that the SPM-induced instabilities can be suppressed by inserting a passive fiber of suitable length inside the laser cavity. The optimum length of the fiber depends, among other things, on the magnitude of round-trip cavity losses and the pumping level at which the laser operates. The stability of YDFL depends on the relative magnitudes of two time scales known as the gain-recovery time and the cavity lifetime. A stable operation occurs when the passive fiber length is long enough to make the cavity lifetime longer than the gain-recovery time.

REFERENCES

[1] I. Kelson and A. A. Hardy, "Strongly pumped fiber lasers," *IEEE J. Quantum Electron.*, vol. 34, no. 9, pp. 1570–1577, Sep. 1998.

[2] Y. H. Tsang, T. A. King, T. Thomas, C. Udell, and M. C. Pierce, "Efficient high power Yb^{3+}-silica fibre laser cladding-pumped at 1064 nm," *Opt. Commun.*, vol. 215, nos. 4–6, pp. 381–387, Jan. 2003.

[3] F. Fontana, M. Begotti, E. M. Pessina, and L. A. Lugiato, "Maxwell–Bloch mode-locking instabilities in erbium-doped fiber lasers," *Opt. Commun.*, vol. 114, nos. 1–2, pp. 89–94, Jan. 1995.

[4] F. Sanchez, P. Le Boudec, P.-L. Francois, and G. Stephan, "Effects of ions pairs on the dynamics of erbium-doped fiber lasers," *Phys. Rev. A*, vol. 48, no. 3, pp. 2220–2229, Sep. 1993.

[5] S. D. Jackson and T. A. King, "Dynamics of the output of heavily Tm-doped double-clad silica fiber lasers," *J. Opt. Soc. Am. B*, vol. 16, no. 12, pp. 2178–2188, 1999.

[6] M. Dinand and C. Schütte, "Theoretical modeling of relaxation oscillations in Er-doped waveguide lasers," *J. Lightw. Technol.*, vol. 13, no. 1, pp. 14–23, Jan. 1995.

[7] R. Rangel-Rojo and M. Mohebi, "Study of the onset of self-pulsing behavior in an Er-doped fiber laser," *Opt. Commun.*, vol. 137, nos. 1–3, pp. 98–102, Apr. 1997.

[8] S. D. Jackson, "Direct evidence for laser reabsorption as initial cause for self-pulsing in three-level fiber lasers," *Electron. Lett.*, vol. 38, no. 25, pp. 1640–1642, Dec. 2002.

[9] F. Brunet, Y. Taillon, P. Galarneau, and S. LaRochelle, "A simple model describing both self-mode locking and sustained self-pulsing in ytterbium-doped ring fiber lasers," *J. Lightw. Technol.*, vol. 23, no. 6, pp. 2131–2138, 2005.

[10] A. Hideur, T. Chartier, C. Ozkul, and F. Sanchez, "Dynamics and stabilization of a high power side-pumped Yb-doped double-clad fiber laser," *Opt. Commun.*, vol. 196, nos. 4–6, pp. 311–317, Dec. 2000.

[11] Y. H. Tsang, T. A. King, D.-K. Ko, and J. Lee, "Output dynamics and stabilization of a multi-mode double-clad Yb^{3+}-doped silica fibre laser," *Optics Commun.*, vol. 259, no. 1, pp. 236–241, Mar. 2006.

[12] W. Guan and J. R. Marciante, "Complete elimination of self-pulsations in dual-clad ytterbium-doped fiber lasers at all pumping levels," *Opt. Lett.*, vol. 34, no. 6, pp. 815–817, 2009.

[13] A. Hardy and R. Oron, "Signal amplification in strongly pumped fiber amplifiers," *IEEE J. Quantum Electron.*, vol. 33, no. 3, pp. 307–313, Mar. 1997.

[14] C. J. Gaeta, M. J. F. Digonnet, and H. J. Shaw, "Pulse characteristics of Q-switched fiber lasers," *J. Lightw. Technol.*, vol. LT-5, no. 12, pp. 1645–1651, Dec. 1987.

[15] P. R. Morkel, K. P. Jedrzejewski, and E. R. Taylor, "Q-switched neodymium-doped phosphate glass fiber lasers," *IEEE J. Quantum Electron.*, vol. 29, no. 7, pp. 2178–2188, Jul. 1993.

[16] D. H. Stone, "Effects of axial nonuniformity in modeling Q-switched lasers," *IEEE J. Quantum. Electron.*, vol. 28, no. 10, pp. 1970–1973, Oct. 1992.

[17] G. P. Agrawal, *Nonlinear Fiber Optics*, 4th ed. Boston, MA: Academic, 2007.

[18] R. Paschotta, J. Nilsson, A. C. Tropper, and D. C. Hanna, "Ytterbium-doped fiber amplifiers," *IEEE J. Quantum Electron.*, vol. 33, no. 7, pp. 1049–1056, Jul. 1997.

[19] E. Desurvire and J. R. Simpson, "Amplification of spontaneous emission in erbium doped single-mode fibers," *J. Lightw. Technol.*, vol. 7, no. 5, pp. 835–845, May 1989.

[20] I. Kelson and A. A. Hardy, "Strongly pumped fiber lasers," *IEEE J. Quantum Electron.*, vol. 34, no. 9, pp. 1570–1577, Sep. 1998.

[21] H. M. Pask, R. J. Carman, D. C. Hanna, A. C. Tropper, C. J. Mackechnie, P. R. Barber, and J. M. Dawes, "Ytterbium-doped silica fiber lasers: Versatile sources for the 1-1.2 μm region," *IEEE J. Select. Topics Quantum Electron.*, vol. 1, no. 1, pp. 2–13, Apr. 1995.

Hojoon Lee (S'78–M'89–SM'09) was born in Seoul, Korea. He received the B.S., M.S., and Ph.D. degrees from the Department of Electronic Engineering, Sungkyunkwan University, Seoul, in 1978, 1980, and 1986, respectively.

He joined the Korea Military Academy, Seoul, in 1980 for 3 years, where he became a full-time Instructor in the Department of Electronic Engineering. In 1987, he joined the Department of Information and Communication Engineering, Hoseo University, Asan, Korea, where he is currently a Professor of Optical Communications. He was a Post-Doctoral Researcher at the Department of Electrical Engineering, Stanford University, Stanford, CA, from 1991 to 1992, and a Visiting Professor at the Institute of Optics, University of Rochester, Rochester, NY, from 2002 to 2003. He has authored or co-authored more than 100 journal and conference papers and has several patents. His current research interests include optical fiber communications, optical fiber sensor systems, fiber Bragg grating fabrication, and nonlinear pulse propagation in fiber gratings.

Govind P. Agrawal (M'83–SM'86–F'96) received the B.Sc. degree from the University of Lucknow, Lucknow, India, in 1969, and the M.Sc. and Ph.D. degrees from the Indian Institute of Technology, New Delhi, India, in 1971 and 1974, respectively.

He joined the faculty of the Institute of Optics, University of Rochester, Rochester, NY, in 1989, where he is currently a Professor of optics. Previously, he held positions in the Ecole Polytechnique, Paris, France, City University of New York, New York, NY, and AT&T Bell Laboratories, Murray Hill, NJ. He is the author or co-author of more than 300 research papers, several book chapters and review articles, and seven books entitled: *Semiconductor Laser* (Norwell, MA: Kluwer Academic, 1993); *Fiber-Optic Communication Systems* (Hoboken, NJ: Wiley, 2002); *Nonlinear Fiber Optics* (Boston: Academic Press, 2007); *Applications of Nonlinear Fiber Optics* (Boston: Academic Press, 2008); *Optical Solitons: From Fibers to Photonic Crystals* (San Diego, CA: Academic Press, 2003); *Lightwave Technology: Components and Devices* (Hoboken, NJ: Wiley, 2004), and *Lightwave Technology: Telecommunication System* (Hoboken, NJ: Wiley, 2005). His current research interests include optical communications, nonlinear optics, and laser physics.

Dr. Agrawal is a Fellow of the Optical Society of America (OSA). He is also a Life Fellow of the Optical Society of India. He has participated multiple times in organizing technical conferences sponsored by the IEEE and the OSA. He was the General Co-Chair in 2001 for the Quantum Electronics and Laser Science Conference and a member of the Program Committee in 2004 and 2005 for the Conference on Lasers and Electro-Optics.